Proceedings of
11th European Conference on Turbomachinery Fluid dynamics & Thermodynamics
ETC11, March 23-27, 2015, Madrid, Spain

Aeroacoustic analysis of a steam turbine double seat control valve

C. Bianchini, R. Da Soghe

Ergon Research s.r.l.
via Panciatichi 92, 50127 Florence, Italy
cosimo.bianchini@ergonresearch.it

E. Imparato, L. Cosi

GE Oil & Gas
via Matteucci 2, 50127 Florence, Italy
enzo.imparato@ge.com

ABSTRACT

A computational analysis of the acoustic response of a double seat valve employed in the control stage of an industrial steam turbine was performed to verify possible criticalities in terms of mechanical stresses. Unsteady CFD was exploited to evaluate the unsteady pressure loads on selected positions. Turbulent flow simulations adopt the Scale Adaptive Simulation principle, as implemented in Ansys CFX 14.5 code, to partially resolve turbulence spectrum. 180 deg symmetric computational models were used, after verification that principal flow features of the full geometry were adequately reproduced, to maintain grid size below 20M cells. Purely acoustic computations exploiting the homogeneous Helmoltz equation were conducted first to identify natural acoustic modes and secondly to verify the forced response subjected to the unsteady pressure loads computed by CFD. Investigated frequency range is extended from 5 to 1000 Hz to comprehend all relevant structural modes. 4 different flow conditions were investigated to represent the entire operating range both in terms of characteristic Reynolds and Mach number. Obtained results shows that principal forcing frequency is characterized by a constant Strouhal number based on plug diameter and bulk flow velocity while main load amplitude is proportional to Reynolds number. Acoustic modes correspond to much higher frequencies so that the forced response does not generate critical stress levels on both valve stem and chest.

NOMENCLATURE

D Valve diameter $[m]$
dt Computational time step $[s]$
dp Mean static pressure loss (inlet-outlet) $[Pa]$
f Characteristic frequency $[s^{-1}]$
H Valve lift $[m]$
k Turbulent kinetic energy $[m^2/s^2]$
l Characteristic length $[m]$
L Discharge duct length $[m]$
L_{RANS} Characteristic turbulent length for RANS models $[m]$
L_{Δ} Characteristic turbulent length based on grid scale $[m]$
$\dot{m}$ Mass flow rate $[kg/s]$
$\dot{m}_c$ Critical mass flow rate $[kg/s]$
Ma Mach number $[-]$
p Static pressure $[Pa]$
R_{ij} Velocity correlations $\overline{u_i' u_j'}$ $[m^2/s^2]$
Re Reynolds number $[-]$
St Strouhal number $[-]$
U Velocity $[m/s]$
u', v', w' x,y,z, directed velocity fluctuations $[m/s]$
ω Turbulent specific dissipation rate $[s^{-1}]$

INTRODUCTION

Design of large and medium scale steam turbine currently needs to address an increasing demand for operational flexibility. This is due to the frequent partialization caused both by the fluctuating availability of renewable power sources, which are ceaselessly enlarging their contribution to the total power generation, and to their use for decentralized purposes or mechanical drive applications which require rapid adjustment to consumption power loads.

These requirements affect the design of most components as many will face off-design conditions for a large part of their lifetime but above all become crucial for the main control valve which regulate the overall pressure ratio available for the steam expansion thus determining the operating conditions of the entire machine.

Clari et al. (2011) and Tecza et al. (2010) propose an innovative control valve design, with respect to standard common lift bar mounting which is prone to oscillating flows possibly leading to plug or stem failures, to reduce or prevent fluid structure interaction causing self-excited vibration in the original design, which protects the control mechanism from the steam flow in the steam chest and through the valve.

Liu et al. (2008) studied the pressure drops across these valves by means of experimental investigation and numerical simulation. Based on the analysis of thermodynamic process in control valve, they deduced a relationship of flow coefficient, area ratio of valve outlet section to seat diameter section, pressure ratio and total pressure loss coefficient with a relative deviations between formula results and experimental results within 3%. They also stated that systematic measurement results indicate that control valve operates steadily when the Mach numbers at valve inlet and outlet sections are less than 0.15 viceversa stem vibration is registered when the pressure ratio is from 0.8 to 0.4.

Also Morita et al. (2004) investigated the problem of stem vibration including both computational and experimental analysis. They performed Large Eddy Simulation of the air flow within a pipe

duct throttled with an emi-sphere plug head which showed to compare well with unsteady pressure measurements on the valve and the valve seats. The analysis was later expanded to include real steam flows finding out that the two gas show the same rotating pressure fluctuations: amplitude of such fluctuations increases with the lift while the propagation frequency decreases Morita and Inada (2007).

More recently Zanazzi et al. (2013) performed a numerical investigation of the unsteady behaviour of steam turbine partition valve in throttling conditions. This work is interesting because they compared a simplified in-house procedure with full 3D CFD analysis and experiments available for a single seat valve with axisymmetric stem under a large number of working conditions which are characterized by 5 different unsteady modes. They were able to reproduce accurately the forcing frequencies despite the fact that pressure amplitudes were strongly underestimated by the CFD procedure.

The aim of present work is to investigate the unsteady forcing acting on the stem and the chest of a double seat valve employed in the regulation of medium sized (up to 80 MW) steam turbine for mechanical drive applications (e.g. oil refinery). In particular it is of interest to verify if the main fluid dynamic modes excite the acoustic natural frequencies to prevent possible resonance phenomena. 3D computations were used to resolve the mean and fluctuating turbulent flow field. Being direct resolution of the turbulent field infeasible with available computational resources for the configuration of interest, an hybrid method based on the Scale Adaptive Simulation technique was exploited to simulate the large scale turbulent structures determining the unsteady aerodynamic loads.

Several operating conditions were analyzed ranging from almost closed shutter with choked flow to fully open valve at maximum flow rate. The unsteady behaviour of the flow is described monitoring pressure signals at various locations and analysing their spectral distribution. Such pressure fluctuations were finally exploited as constraints to compute the forced acoustic internal field.

Similar analysis, showing the high interest of scientific community in the characterization of the unsteady valve behaviour, have been recently presented by Musch et al. (2014) and Domnick et al. (2014) employing equivalent numerical techniques.

INVESTIGATED CASES

This paper is focused on the double seat valve depicted in Figure 1. This valve is composed by a radial admission duct which feeds the axial turbine through two annular orifices regulated by means of the same two-plug stem. The lower seat directly admits the steam to the main discharge duct while the upper one is collected by a spiral which surrounds the internal steam chest.

This valve is investigated with the stem opened at three different heights above the seat (H/D = 0.040, 0.153, 0.404), representing two start-up configurations and full load positioning. In terms of

Table 1: Investigated cases

	Inlet Mach 10^{-2}	**Inlet Reynolds** 10^{6}	**H/D**
Case 1	1.948	10.96	0.040
Case 2	7.353	41.24	0.153
Case 3	9.105	53.64	0.404
Case 4	13.206	64.55	0.404
Case 5	9.376	24.27	0.404
Case 6	14.064	85.67	0.404

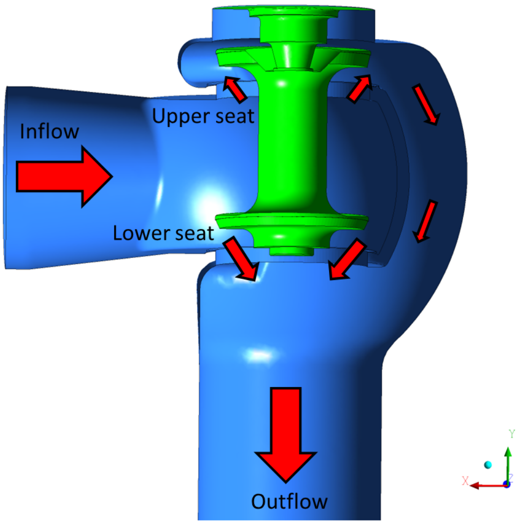

Figure 1: Overview of double seat valve geometry.

flow conditions the two closed plug cases were investigated with a large pressure drop generating fully choked throats as encountered in standard start-up procedure. The wide open valve configuration instead is employed under a variety of conditions among which 4 different simulations were performed to well represent the entire range of interest. A summary of investigated flow conditions is reported in Table 1 as a function of inlet Mach and Reynolds number and stem positioning.

An overview of the effective flow conditions which the valve may be subjected is summarized in Figure 2 in terms of inflow Mach and Reynolds numbers where dots indicate the cases investigated in this analysis reported in Table 1.

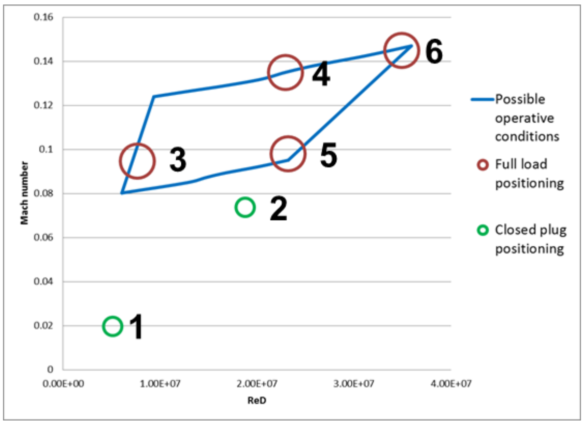

Figure 2: Possible operating conditions.

NUMERICAL METHODS

As better reported in Bianchini et al. (2014), this analysis, based on the procedure proposed and validated by Zanazzi et al. (2013), exploits the $k-\omega$ SST SAS model in the version implemented within the commercial CFD code Ansys® CFX v14.5.

In terms of modelling it is worth recalling that steam is treated as a homogeneous rarefied gas

following ideal gas law. Despite being substantially isothermal, total energy equation was solved with adiabatic conditions on all the walls to consider thermal gradients generated due to the acceleration within the valve throat which in the choked cases is quite relevant.

A physical time step $dt = 1e^{-4}$ was chosen based on physics and computational efficiency considerations. Convergence was guaranteed for each time step by RMS residuals for continuity and momentum below 10^{-5}. To obtain converged statistics and maximise the investigated spectra, total simulation time was extended over 0.4 s for a total of more than 4000 time steps. Transient effects due to initialization were purged activating time averaging and signal monitoring after 0.2 s. As it is desired for direct resolution of turbulent flows, highest available order of discretization (2^{nd} order as typical for unstructured codes) for both convective and time advancement terms are used exploiting the high resolution formulation to improve solver robustness.

The computational domain employed in this analysis extends in the upstream direction up to the steam chest inflow section while downstream the discharge duct is extruded for $L > 10D$ to avoid backflow or any interaction with the boundary condition.

Even though in principle for turbulent flows the use of symmetry conditions should always be avoided as the flow is symmetric only in a time averaged sense while the instantaneous flux across the plane of symmetry is not zero, it would be convenient to force the symmetric behavior by means of boundary conditions to reduce the computational cost. In order to verify the applicability of this assumption, the full $360°$ geometry was simulated for Case 1 showing that the flow field within the valve exhibits an almost symmetrical behavior not only in terms of time averaged flow field but also in terms of turbulent fluctuations as demonstrated in Bianchini et al. (2014).

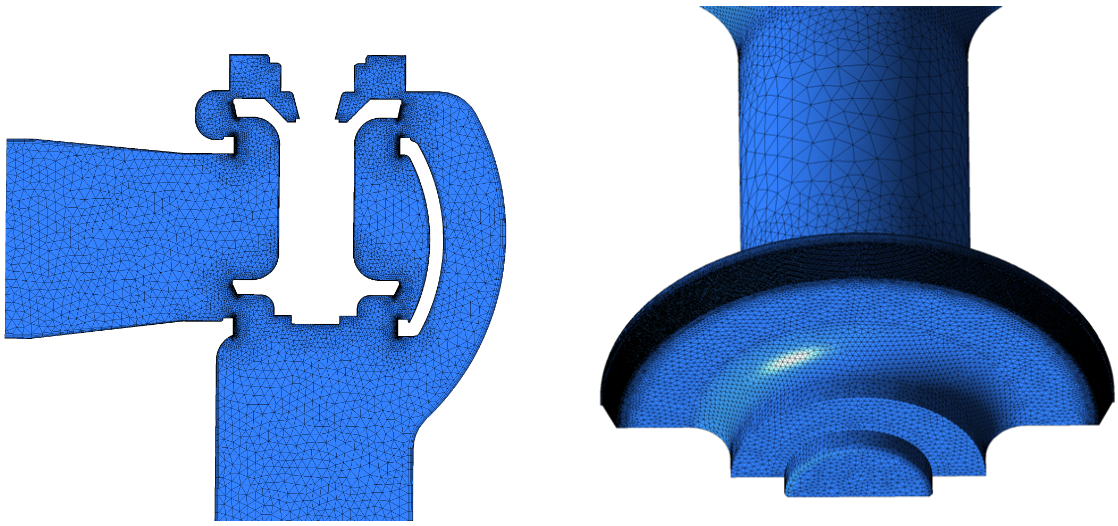

(a) Details of computational grid on symmetry plane

(b) Details of computational grid on valve stem

Figure 3: Overview of computational grid.

The three employed meshes are generated using same procedures and criteria: hybrid element shape, i.e. tetrahedra in the free stream with 5 layers of prisms along the walls to discretize boundary layer, and fine grid clustering in the throat and on the stem. Near wall grid size is chosen to maintain first node dimensionless wall distance y^+ below 300 to fulfil wall function requirements on most of the walls and in particular in the proximity of the throttling section. Meshes count approximately 14M cells distributed as depicted in Figure 3 to maintain an adequate grid size also in the far field region

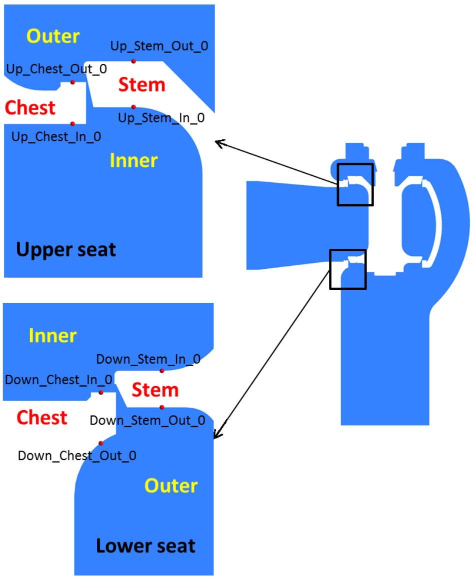

Figure 4: Pressure probe positioning.

to permit a sufficient resolution of the turbulent flow field. Employed grids guarantee high quality elements as the averaged orthogonality angle is above $70°$ and the mesh expansion factor below 3.

Data analysis

The synthesis of 3D computations of turbulent flows in values useful to characterize the unsteady behavior of the fluid is not always straightforward due to both the large number of data produced and the chaotic nature of turbulence which makes the analysis of principal flow structures a challenging task. In this case for example, the work is dedicated to an estimate of the fluctuating aerodynamic forcing acting on the stem and the steam chest to verify possible interaction with the structure eigenmodes. The idea of collecting instantaneous pressure fields on all computational nodes of the surfaces of interest for the entire simulated time is not practical. Apart from problems arising due to the size of the dataset, time signals contains contributions pulsating at different frequencies which are difficult, virtually impossible, to analyze in the time domain.

In order to completely characterize the main forces acting on the valve in a light and simple way, pressure signal is registered in a reduced set of nodes together with global forces and moments acting on the stem. Most interesting locations were identified on overhung structures such as the stem plug and the chest narrowing. As depicted in Figure 4, 8 different positions were selected to be representative of pressure loads on the shutter and on the external structure; for each position 9 probes were distributed tangentially with a spacing of $22.5°$ for a total of 72 pressure signals registered. To more easily identify the monitor points they are named with a composite word identifying nearest seat (Up/Down), closest surface (Stem/Chest), relative position respect to the valve throat (In/Out) and finally the angular coordinate (e.g $Up\_Stem\_Out\_45$). Discrete Fourier Transform was hence applied to every local signal permitting to highlight principal frequencies, relative phase of fluctuations, interactions between different zones of the domain.

With the above mentioned numerical set-up, frequencies ranging between 5 and 5000 Hz are analyzed providing a sufficient resolution to properly characterize the range of interest (10-1000 Hz).

UNSTEADY LOADS

In order to analyze such a huge number of data to extract information on the global behaviour of the unsteady steam flow within the valve, Discrete Fourier Transform of registered pressure signals was exploited as main tool. As an example, frequency spectra of probes located at two representative locations (Up_Chest_Out and $Down\_Stem\_In$) are reported in Figures 5 and 6 for each case. Different curves corresponds to different tangential positions, black lines reports the natural eigenfrequencies identified in the acoustic analysis: such values are available for the open valve cases only.

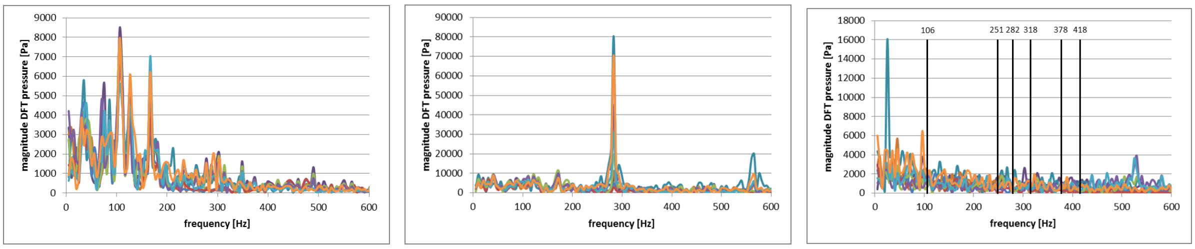

(a) Case 1 (b) Case 2 (c) Case 3

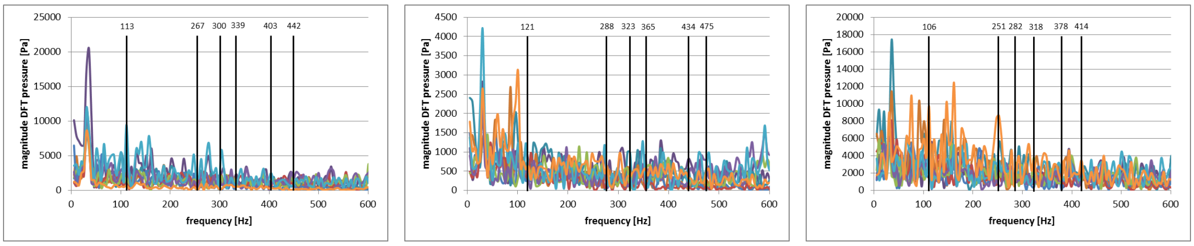

(d) Case 4 (e) Case 5 (f) Case 6

Figure 5: Amplitude DFT pressure signal on Up_Chest_Out probes.

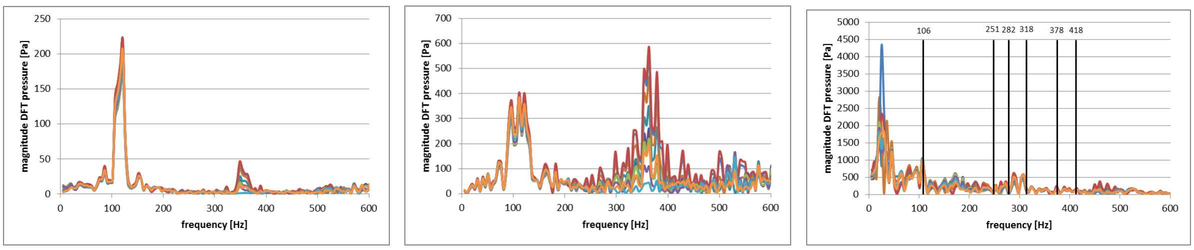

(a) Case 1 (b) Case 2 (c) Case 3

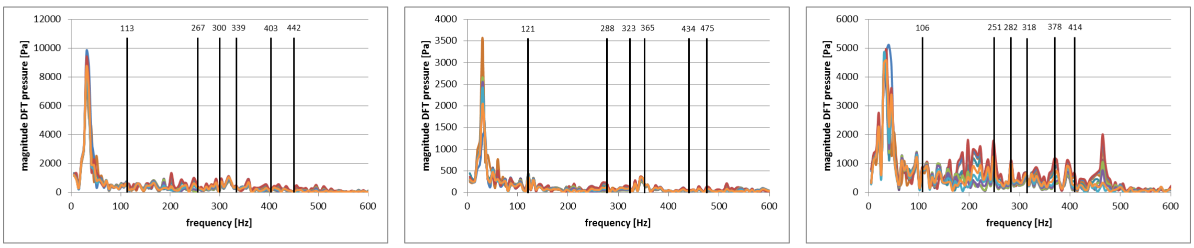

(d) Case 4 (e) Case 5 (f) Case 6

Figure 6: Amplitude DFT pressure signal on $Down\_Stem\_In$ probes.

The internal fluctuations, i.e. Figure 6, are characterized by a lower broadband contribution and main peaks are clearly identifiable. The external ones, i.e. Figure 5, viceversa present higher peak amplitudes and a larger spread on frequency band: significant contributions are however limited for all probes, and for each investigated case, in the range 10-1000 Hz. An exception to this general trend seems Case 2, reported in Figures 5(b) and 6(b), but only due to the very large pressure fluctuations which arise outside the inner chamber reaching values as high as 80 kPa. Furthermore the pressure signals at the various probes along the same circumference are consistent with eachother with perfectly matching peak frequency and only slight deviations in the amplitude. Comparison with obtained acoustic eigenfrequencies, superposed to pressure spectra in Figures 5 and 6, shows a substantial decoupling between acoustic and fluid dynamic characteristic frequencies as first natural modes appear above 100 Hz while the forcing frequency is much lower. Despite acoustic eigenfrequency could not be computed directed for the choked cases because of the loss in accuracy of the acoustic computational method, it is possible to see how the principal forcing frequencies for Case 1 and 2 are very close to obtained first longitudinal mode for the other cases. Being that frequency almost invariant to operating condition, such peaks are hence probably due to the influence of acoustics on fluid dynamic for Case 1 and 2.

It is interesting to extract from the obtained spectra, also those not shown here for the sake of clarity, a characteristic frequency both for inner and outer probes. This characteristic frequency is intended as the lowest frequency characterized by a significant peak which stands out against background pressure level in the neighbourhood and is registered for most tangentially distributed probes. These obtained principal frequencies are reported in Table 2 showing how, for subsonic cases at least, throat acceleration is not sufficient to acoustically decouple upstream and downstream region. For Cases 3 to 6 in fact internal and external frequencies are equal and present very small variations around the same value, while in Cases 1 and 2 outer probes are more independently fluctuating showing in one case slightly lower characteristic frequency and in the other a value higher than second harmonic.

Since the obtained frequencies for the inner probes can be roughly grouped in two homogeneous subset characterized respectively by values around 115 Hz for the choked cases and 30 Hz for the subsonic cases, it would be convenient to use the performed run to propose a simple model based on geometry and flow conditions only to provide a first estimate of the characteristic frequency of the fluid forcing which may help at early design stage. In order to understand which may be the relevant parameters, a set of characteristic velocities and lengths are combined together to calculate various dimensionless expressions defined as Strouhal numbers $St = l \cdot f/U$. In particular for the velocity both the sound speed (acoustic) and the bulk steam velocity in throat (aero) have been used, while in terms of length scales the upper and lower throat gaps as well as the stem diameter were

Table 2: Principal frequencies

	Inner probes [Hz]	**Outer probes** [Hz]
Case 1	116	106
Case 2	113	280
Case 3	25	25
Case 4	30	30
Case 5	30	30
Case 6	35	35

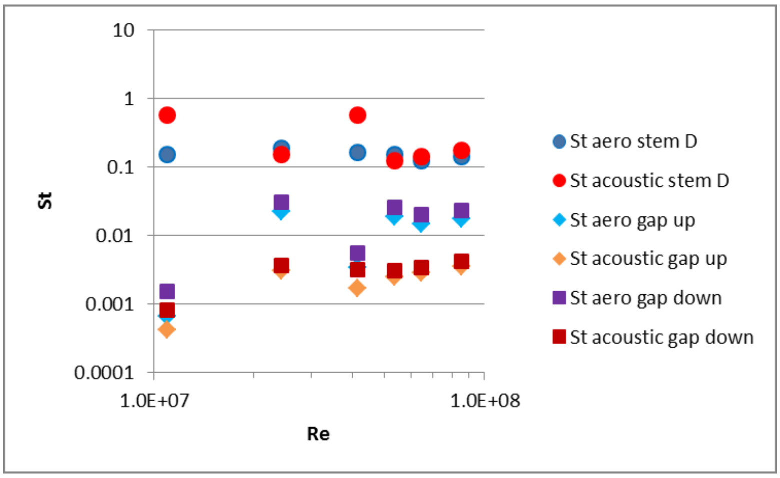

Figure 7: Strouhal number evaluation for inner probes.

employed. In such a way 6 different Strouhal may be computed as plotted in Figure 7 in a log-log graph for the inner probes. It is worth noting how the only Strouhal showing results of the same order of magnitude for every tested conditions is that defined on the aerodynamic velocity in the throat and the stem diameter. With a constant St=0.15, obtained averaging the 6 investigated cases, it is possible to evaluate characteristic internal frequencies with an average error of 10% which is generally compatible with safety coefficients employed by structural designers to avoid dangerous interactions with structure eigenfrequencies.

Also in terms of peak amplitudes, the two groups of subsonic and choked cases behave differently. For the supersonic cases in fact, the inner chamber is almost steady while the amplitude of fluctuations due to the annular jet is large reaching values higher than 40 kPa as a tangential average, resulting nearly 4 times higher than in the most critical subsonic case. The subsonic cases viceversa show as expected a stronger link between internal and external oscillation magnitude: outer fluctuations are limited to nearly the double of their respective upstream homologous. In order to provide a description of how these pressure fluctuations depends on the operating conditions and on the probe position, maximum Fourier coefficient was averaged tangentially for each position and plotted in Figure 8

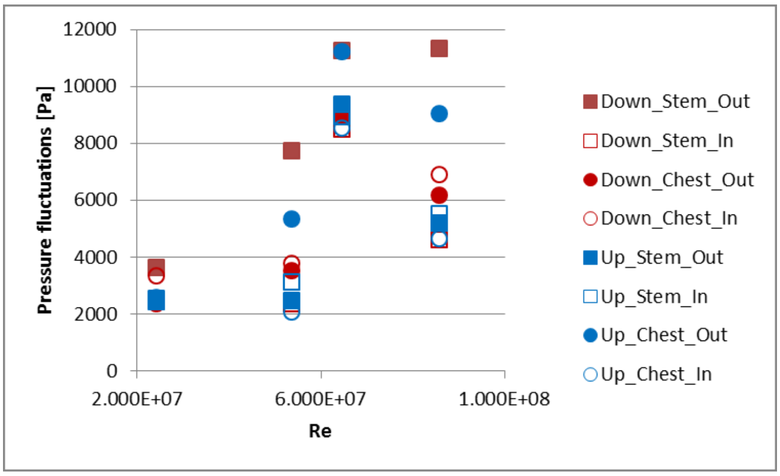

Figure 8: Fluctuation amplitudes for subsonic cases.

against Reynolds number for the subsonic cases. Lower seat is subjected to higher unsteady loads than the upper one, in particular those directed on the stem of the valve which shows an increasing trend with Reynolds number. This fluctuation is propagated towards the other probe positions with attenuation proportional to fluid reference density which regulates flow inertia. As a consequence Case 3 and 6, which correspond to $Re = 5.36 \cdot 10^7$ and $8.57 \cdot 10^7$ respectively, results in lower minimal oscillation. It is interesting to note that the upper seat, due to its shaping, excites the chest much more than the stem.

ACOUSTIC ANALYSIS

In order to verify that the computed aerodynamic forcing was not capable of exciting any acoustic mode of the valve, hence mitigating the risk for self generated acoustic interactions possibly leading to rupture due to resonance effects, FEM analysis was exploited to perform both natural and forced acoustic response of the valve in open plug conditions.

The homogeneous Helmoltz equation is solved by means of Ansys mechanical commercial solver neglecting mean flow effects and assuming linear elastic perfect gas behaviour. The assumption of neglecting the mean flow effects in the acoustic analysis is justified noticing that Mach number within the entire domain is quite low. The acoustic analysis was thus performed for the open-valve conditions only where actual pressure wave velocity is not deeply affected by the mean aerodynamic flow also through valve throat. First 6 obtained natural acoustic modes at working conditions corresponding to case 3 are reported in Figure 9 showing that the acoustic forcing frequency around 30 Hz is well below minimal natural frequency identified at 106 Hz. These results were obtained with acoustic soft boundary conditions imposed on inlet and outlet, however may be considered general as a sensitivity

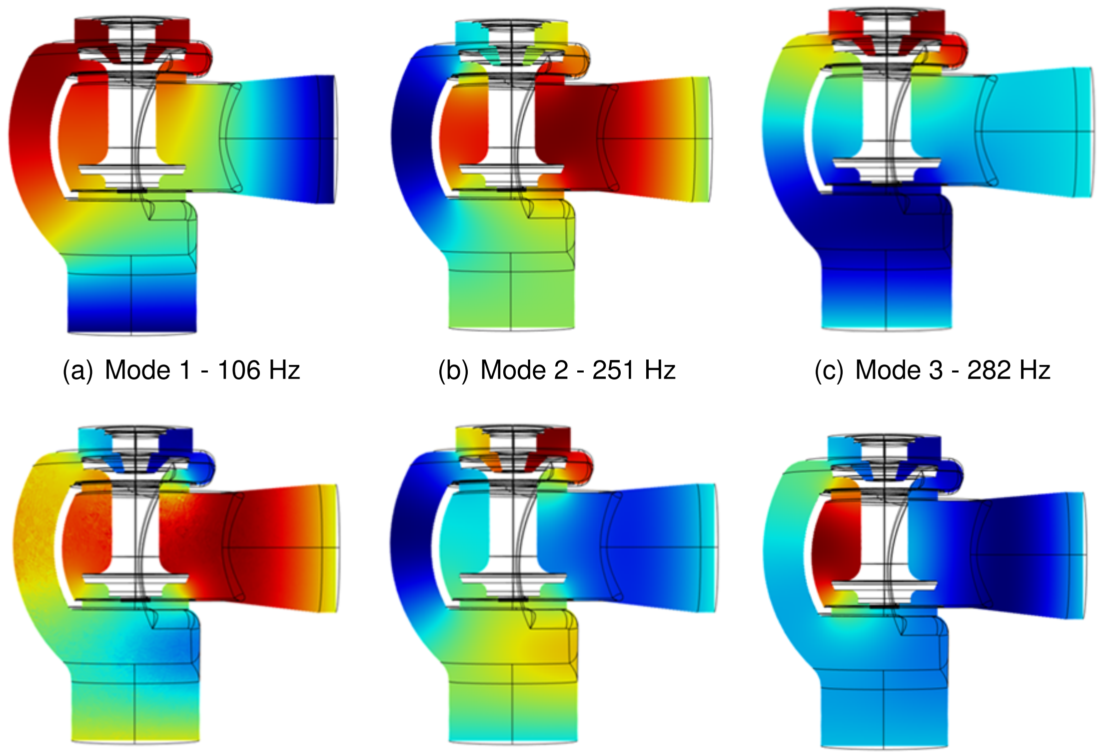

(a) Mode 1 - 106 Hz (b) Mode 2 - 251 Hz (c) Mode 3 - 282 Hz

(d) Mode 4 - 319 Hz (e) Mode 5 - 378 Hz (f) Mode 6 - 414 Hz

Figure 9: First 6 natural acoustic modes.

analysis showed low changes in case of hard sound boundary. All solid walls are modelled as sound hard boundary.

Fourier transformed pressure history at monitored probes were then used to perform a forced acoustic analysis. DOF constraints were imposed on the closest nodes of the FEM mesh to respect real and imaginary components of pressure DFT. Based on the previous natural modes, locations prone to high amplitude fluctuations were selected (max and mean peak value for each mode) and monitored in the entire range of investigated frequencies.

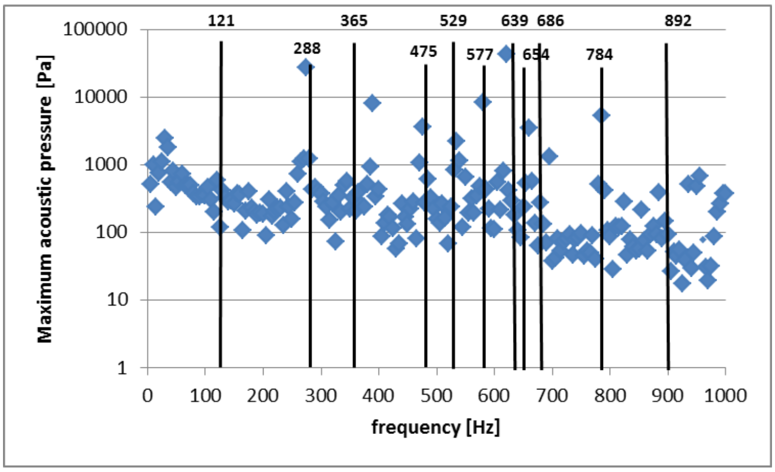

Figure 10: Maximum acoustic pressure magnitude for Case 5.

Figure 10 shows the maximum absolute value of acoustic pressure registered on the critical points of modes 1 to 6. Case 5 is chosen as an example; for each peak the corresponding closest acoustic natural eigenfrequency is superposed to highlight which mode may be excited. Obtained maximum pressure fluctuations are below 1 bar, which is not critical from a structural point of view, for all investigated frequencies. The frequency peak identified at 275 Hz is characterized by low magnitude aerodynamic forcing but sufficiently strong to excite a proper mode, found at 288Hz in the unforced analysis, with modal shape equivalent to that reported in Figure 9(b). All subsequent peaks correspond to other acoustic mode, only first peak does not correspond to any acoustic mode: it corresponds to the peak in generated pressure fluctuations discussed in Unsteady Loads section.

CONCLUSIONS

An unsteady CFD analysis was performed to analyze the oscillating aerodynamic loads acting on the stem and the chest of a double seat partition valve operating upstream the impulse stage of an industrial steam turbine of medium size. Actual geometries and representative flow conditions, ranging from choked throat to open valve configurations, have been considered. The analysis was carried out exploiting hybrid turbulence modelling based on the Scale Adaptive Simulation principle. Unsteady forces are extracted monitoring time signal at selected points to perform spectral decomposition.

Obtained results permitted to identify different behaviours for the subsonic and the choked conditions both in terms of main frequencies and amplitude of oscillations. Coherent fluctuations are observed inside and outside steam chest in the subsonic cases, when the throat is sonic instead inner pressure oscillations are very low while outer gets amplified due to the higher annular jet momentum. In terms of principal frequencies, Strouhal number based on bulk flow velocity and stem diameter is invariant among the investigated cases. It can hence be used to extend obtained findings to other operating conditions predicting a priori proper frequency of the aerodynamic forcing. This information

is useful to guarantee from the early design stage the decoupling between aerodynamic, acoustic and structural eigenfrequency.

Finally acoustic analysis was exploited to verify that maximum sound pressure within the valve were maintained below acceptable levels from a mechanical point of view when subjected to the predicted fluctuating loads.

REFERENCES

C. Bianchini, R. Da Soghe, E. Imparato, and L. Cosi. Numerical analysis of the unsteady loads on a steam turbine double seat control valve. *ASME Conference Proceedings*, 2014(26982), 2014.

Manuel B. Clari, Thomas Polklas, and Franz Joos. Three-dimensional flow separations in the diffuser of a steam turbine control valve. *ASME Conference Proceedings*, 2011(54679):2327–2334, 2011.

C. B. Domnick, F. K. Benra, H. J. Dohmen, and C. Musch. Numerical investigation on the time-variant flow field and dynamic forces acting in steam turbine inlet valves. *ASME Conference Proceedings*, 2014(25632), 2014.

Guanwei Liu, Shunsen Wang, Hui Guo, Jingru Mao, Zhenping Feng, and Xiaowei Xiang. Investigation on flow characteristics and stability of control valves for steam turbines. *ASME Conference Proceedings*, 2008(43154):811–820, 2008.

Ryo Morita and Fumio Inada. Pressure fluctuations around steam control valve: Steam experiments and CFD calculations. *ASME Conference Proceedings*, 2007(26444):421–427, 2007. doi: 10.1115/PVP2007-26444. URL `http://link.aip.org/link/abstract/ASMECP/v2007/i42827/p421/s1`.

Ryo Morita, Fumio Inada, Michitsugu Mori, Kenichi Tezuka, and Yoshinobu Tsujimoto. CFD calculation and experiments of unsteady flow on control valve. *ASME Heat Transfer Fluids Engineering Summer Conference*, 2004(HT-FED04-56017), 2004.

C. Musch, F. Deister, G. Zimmer, I. Balkowski, P. Bruggemann, and W. Haslinger. A new emergency-stop and control-valve design part 2: Validation of numerical model and shape optimization. *ASME Conference Proceedings*, 2014(25117), 2014.

Joseph Tecza, Gocha Chochua, and Randy Moll. Analysis of fluid-structure interaction in a steam turbine throttle valve. *ASME Conference Proceedings*, 2010(44021):2329–2338, 2010.

Giorgio Zanazzi, Ottmar Schaefer, Colin Ridoutt, and Michael Sell. Unsteady CFD simulation of control valve in throttling conditions and comparison with experiments. *ASME Conference Proceedings*, 2013(94788), 2013.